Microwave Impedance Measurement for Nanoelectronics

Martin RANDUS, Karel HOFFMANN

Dept. of Electromagnetic Field, Czech Technical University in Prague, Technicka 2, 166 27 Prague, Czech Republic

randumar@fel.cvut.cz, hoffmann@fel.cvut.cz

Abstract. *The rapid progress in nanoelectronics showed an urgent need for microwave measurement of impedances extremely different from the 50Ω reference impedance of measurement instruments. In commonly used methods input impedance or admittance of a device under test (DUT) is derived from measured value of its reflection coefficient causing serious accuracy problems for very high and very low impedances due to insufficient sensitivity of the reflection coefficient to impedance of the DUT. This paper brings theoretical description and experimental verification of a method developed especially for measurement of extreme impedances. The method can significantly improve measurement sensitivity and reduce errors caused by the VNA. It is based on subtraction (or addition) of a reference reflection coefficient and the reflection coefficient of the DUT by a passive network, amplifying the resulting signal by an amplifier and measuring the amplified signal as a transmission coefficient by a common vector network analyzer (VNA). A suitable calibration technique is also presented.*

Keywords

Calibration, impedance measurement, microwave circuits, microwave measurements, nanotechnology.

1. Introduction

A rapid progress in the field of nanoelectronics with application of carbon nanotubes as the key elements for future high-speed devices showed an urgent need for broadband microwave measurement of extreme impedances – input impedances that are significantly higher or significantly lower than a reference impedance of a measurement system, that is usually $Z_0 = 50$ Ω. A typical input impedance of carbon nanotube devices is usually in orders of tens and hundreds of kΩ [1], [2]. On the other hand, high-speed digital systems need power delivery networks with extremely low impedance in orders of mΩ [3].

Classical method of impedance measurement based on measuring of a reflection coefficient of a device under test (DUT) by a vector network analyzer (VNA) and subsequent calculating of input impedance Z_x of the DUT [4] as

$$Z_x = Z_0 \frac{1 + \Gamma_x}{1 - \Gamma_x} \tag{1}$$

suffers from serious inaccuracy issues for very high and very low impedances due to loosing reflection coefficient sensitivity to impedance value [5]. This can be clearly seen from Fig. 1, where the value of the reflection coefficient Γ_x saturates for high and low input impedances $Z_x = R_x + j0$.
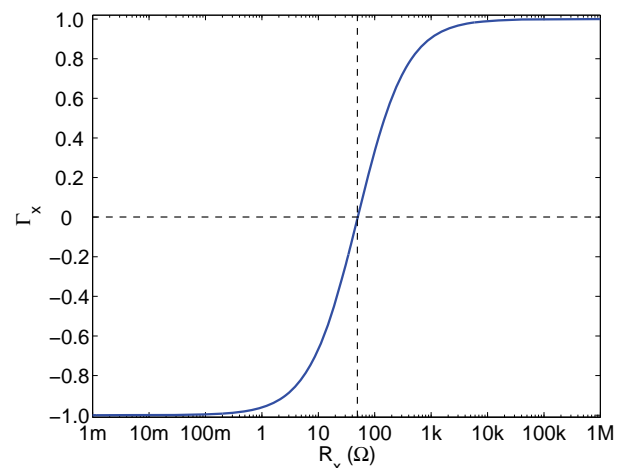
Fig. 1. Dependence of the reflection coefficient Γ_x on the value of purely real impedance $Z_x = R_x + j0$ of the DUT. Sensitivity of the reflection coefficient Γ_x to impedance Z_x rapidly decreases for very high impedances ($R_x > 10$ kΩ for $\Gamma_x > 0.99$) and for very low impedances ($R_x < 250$ mΩ for $\Gamma_x < -0.99$).

This paper brings theoretical description and experimental verification of a measurement method developed especially for measurement of extreme impedances. The method may be used either for measurement of high impedances or for measurement of low impedances. A new calibration technique suitable for measurement of extreme impedances is also provided.

2. Theory

For simplicity, the basic principle of the proposed measurement method will be explained on an idealized measurement system composed of ideal components. Subsequently, a suitable error model and a calibration technique for a real measurement system will be described.

2.1 Ideal Case

An arrangement of an idealized measurement system implementing the developed method is depicted in Fig. 2, where a_1 is the source (incident) normalized wave and b_2 is the received normalized wave, defined as it is common for scattering parameters definition [6], Γ_{ref} is a reference reflection coefficient of the reference impedance Z_{ref}, Γ_x is the reflection coefficient of the input impedance Z_x of the DUT and G is voltage gain of the amplifier.
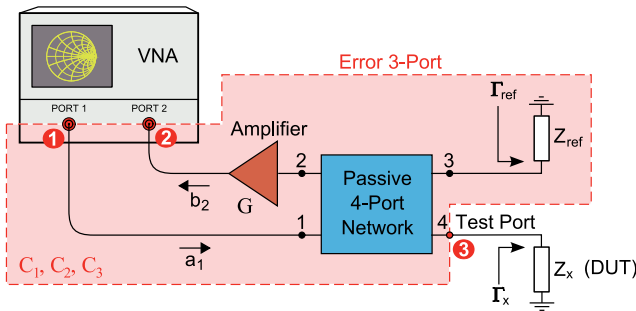
Fig. 2. Arrangement of the measurement system depicted with an error 3-port.

The method is based on adding or subtracting of the reference reflection coefficient ($|\Gamma_{ref}| \approx 1$) to/from the reflection coefficient of the DUT ($|\Gamma_x| \approx 1$) by the passive 4-port network in order to obtain a small output signal, amplifying this small signal by a high-gain amplifier and measuring the resulting signal by a common VNA as a transmission coefficient T_{21}.

In ideal case the transmission coefficient T_{21} from port 1 to port 2 of the VNA is given either as

$$T_{21} = \frac{b_2}{a_1} = \frac{G}{A}\left(\Gamma_x + \Gamma_{ref}\right) \tag{2}$$

in the case of an adding passive 4-port network or as

$$T_{21} = \frac{b_2}{a_1} = \frac{G}{A}\left(\Gamma_x - \Gamma_{ref}\right) \tag{3}$$

in the case of a subtracting passive 4-port network. The complex constant A represents coupling ratios and losses in the passive 4-port network.

Two typical examples of the passive 4-port network are depicted in Fig. 3. The 90degree 3dB hybrid coupler is an adding passive 4-port network with $A = j2$, whereas the 180degree 3dB hybrid coupler is a subtracting 4-port network with $A = 2$.
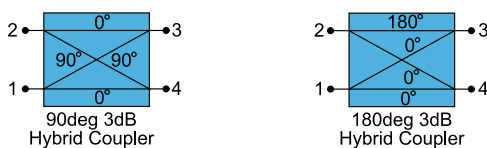
Fig. 3. Typical example of an adding passive 4-port network – the 90degree 3dB hybrid coupler (left) and of a subtracting passive 4-port network – the 180degree 3dB hybrid coupler (right).

To explain the principle of operation of the measurement system in more detail let us now assume e.g. the subtracting passive 4-port network. The equation (3) can be decomposed as

$$T_{21} = T_{21a} - T_{21b} \tag{4}$$

where

$$T_{21a} = \frac{G}{A}\Gamma_x, \tag{5}$$

$$T_{21b} = \frac{G}{A}\Gamma_{ref}. \tag{6}$$

A geometrical interpretation is illustrated in Fig. 4 for the case of subtracting passive 4-port network with $A = 2$ and $G = 1$. This is a typical example when the 180degree 3dB hybrid coupler is used alone without the amplifier.
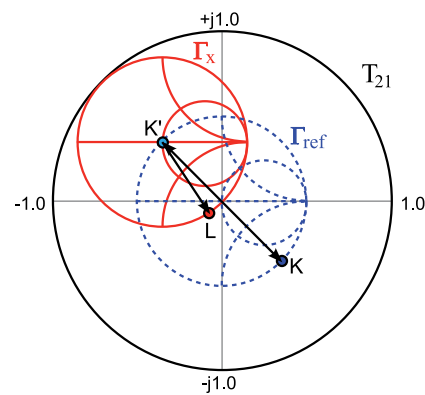
Fig. 4. Graphical representation of equation (3), respectively (4), for the case $A = 2$, $G = 1$ (i.e. the 180degree 3dB hybrid coupler with no amplifier). Point K represents the reference reflection coefficient Γ_{ref} and point K' represents -Γ_{ref} both depicted in the Smith chart Γ_{ref}. Point L represents the reflection coefficient Γ_x of the DUT depicted in the Smith chart Γ_x and it also stands for the actual measured value of the transmission coefficient T_{21} depicted in the complex plane T_{21}.

Equation (6) represents a mapping of the Smith chart Γ_{ref} for the reference impedance to the complex plane of the transmission coefficient T_{21} as it is depicted in Fig. 4. The Smith chart is situated in the center of the complex plane T_{21} and it is scaled by factor $G/A = 0.5$. Point K stands for the chosen reference reflection coefficient Γ_{ref} depicted in this corresponding Smith chart and point K' similarly stands for -Γ_{ref}.

Equation (5) represents a similar mapping of the Smith chart Γ_x for the input impedance of the DUT to the complex plane of the transmission coefficient T_{21}. The Smith chart is also scaled by factor $G/A = 0.5$. The equation (5) locates the Smith chart Γ_x to the center of the complex plane T_{21}. However, in the case of the full equation (4) it is shifted by vector -T_{21b}. Therefore, the center point of the Smith chart Γ_x is situated in the point K'. Point L stands for the reflection coefficient Γ_x of the DUT depicted in the Smith chart Γ_x. Moreover, this point also represents the actual value of the measured transmission coefficient in the complex plane T_{21}.

It is obvious that the reflection coefficients Γ_x of the DUT similar to the reference reflection coefficient Γ_{ref} ($\Gamma_x \approx \Gamma_{ref}$) are mapped by (3) (respectively (4)) near the center of the complex plane T_{21}, i.e. magnitude of the corresponding transmission coefficient T_{21} is very small. That makes possible to amplify the small output signal by a high-gain amplifier.

Now, let us employ an amplifier to amplify the output signal. Supposing that the voltage gain of the amplifier is e.g. $G = 4$ (12 dB) the situation depicted in Fig. 4 changes to the situation depicted in Fig. 5. The both Smith charts Γ_x and Γ_{ref} are scaled up four times leading to increased sensitivity of the measured transmission coefficient T_{21} (point L) to the reflection coefficient Γ_x of the DUT.
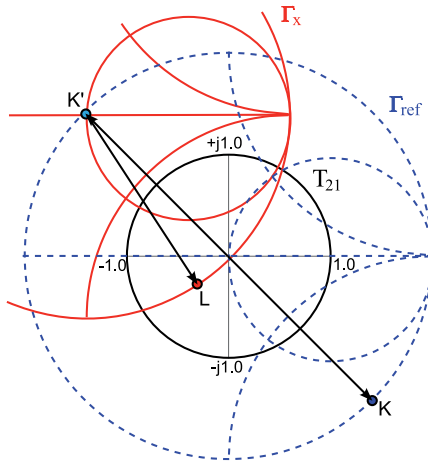
Fig. 5. Graphical representation of equation (3), respectively (4), for the case $A = 2$, $G = 4$ (i.e. the 180degree 3dB hybrid coupler with amplifier of 12dB gain). Point K represents the reference reflection coefficient Γ_{ref} and point K' represents -Γ_{ref} both depicted in the Smith chart Γ_{ref}. Point L represents the reflection coefficient Γ_x of the DUT depicted in the Smith chart Γ_x and it also stands for the actual measured value of the transmission coefficient T_{21} depicted in the complex plane T_{21}.

The sensitivity can be increased simply by applying higher gain G. However, there is a limit for the maximal applicable gain of the amplifier due to nonlinearity of the amplifier and of the receiver in the VNA.

Fig. 6 corresponds to application of the 90degree 3dB hybrid coupler (i.e. the adding passive 4-port network with $A = j2$, equation (2)). The both Smith charts are rotated due to the -90degree phase shifts. Point K stands for the chosen reference reflection coefficient Γ_{ref} depicted in the Smith chart Γ_{ref} and point K' similarly stands for -Γ_{ref}. Point L stands for the reflection coefficient Γ_x of the DUT depicted in the Smith chart Γ_x and it also represents the actual value of the measured transmission coefficient in the complex plane T_{21}. The center of the Smith chart Γ_x is now shifted to point K that is caused by adding properties of the passive network. The measured transmission coefficient T_{21} is small if the reflection coefficients Γ_x of the DUT is similar to the opposite value of the reference reflection coefficient -Γ_{ref} ($\Gamma_x \approx -\Gamma_{ref}$).
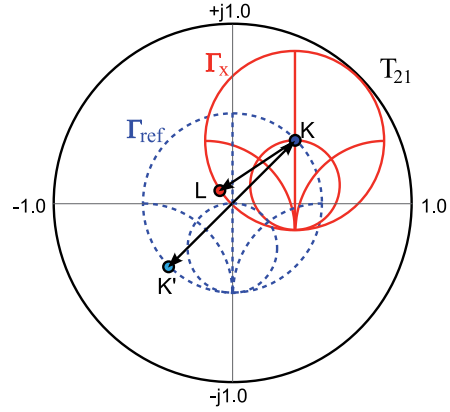
Fig. 6. Graphical representation of equation (2) for the case $A = j2$, $G = 1$ (i.e. the 90degree 3dB hybrid coupler with no amplifier). Point K represents the reference reflection coefficient Γ_{ref} and point K' represents -Γ_{ref} both depicted in the Smith chart Γ_{ref}. Point L represents the reflection coefficient Γ_x of the DUT depicted in the Smith chart Γ_x and it also stands for the actual measured value of the transmission coefficient T_{21} depicted in the complex plane T_{21}.

The improved sensitivity of the proposed method significantly reduces uncertainty of the VNA itself caused by noise and drift. In ideal case the reflection coefficient Γ_x of the DUT from (2) and (3) is given as

$$\Gamma_x = \frac{A}{G}T_{21} \mp \Gamma_{ref} \qquad (7)$$

where the sign depends on the type of the passive 4-port network (adding or subtracting). Noise and drift of the VNA cause that the measured value of the transmission coefficient T_{21} is changed by ΔT_{21}. This causes an error $\Delta\Gamma_x$ of the calculated reflection coefficient Γ_x as

$$\Gamma_x + \Delta\Gamma_x = \frac{A}{G}\left(T_{21} + \Delta T_{21}\right) \mp \Gamma_{ref} . \qquad (8)$$

If we subtract (7) from (8) we see that

$$\Delta\Gamma_x = \frac{A}{G}\Delta T_{21}, \qquad (9)$$

i.e. the error of the VNA ΔT_{21} is reduced G/A-times. Therefore, higher gain of the amplifier G brings better reduction of the measurement uncertainty of Γ_x and thus better determination of Z_x from (1).

The reference reflection coefficient is in practical applications usually open end ($\Gamma_{ref} = 1$) or short ($\Gamma_{ref} = -1$), since these terminations are the easiest for broadband realization. The choice

$$\Gamma_{ref} = -\Gamma_x \qquad (10)$$

in the case of an adding 4-port network and

$$\Gamma_{ref} = \Gamma_x \qquad (11)$$

in the case of a subtracting 4-port network would in ideal case lead to the smallest possible output signal, since $T_{21} = 0$. However, open end or short terminations are

sufficient because for extreme impedances the reflection coefficient of the DUT $|\Gamma_x| \approx 1$.

If e.g. the subtracting 4-port network is used it is possible to measure high impedances if the reference impedance is open end and low impedances if the reference impedance is short. A complete list of applicable measurement system setups is in Tab. 1.

Setup	Passive Network	Γ_{ref}	Z_x
A	Adding	Open	Low
B	Adding	Short	High
C	Subtracting	Open	High
D	Subtracting	Short	Low

Tab. 1. Complete list of measurement system setups – the column Z_x indicates what input impedances of the DUT can be measured with the current setup – 'High' means $Z_x \gg Z_0$ and 'Low' means $Z_x \ll Z_0$.

2.2 Real Components – Calibration

In the real case imperfections of the components of the measurement system must be characterized using a suitable calibration technique and an error model.

The simplest error model that describes the parts of the measurement system highlighted in Fig. 2, including imperfections of the VNA itself (gain tracking error, crosstalk, etc.), is an error 3-port depicted in Fig. 7.

The reference impedance is an integral part of the error 3-port. Therefore, its exact numerical value does not need to be known for calculations, since it is characterized during the calibration process.

By using the error 3-port in Fig. 7 the measured transmission coefficient T_{21} can be calculated as

$$T_{21} = \frac{b_2}{a_1} = \frac{e_{21} + (e_{31}e_{23} - e_{21}e_{33})\Gamma_x}{1 - e_{33}\Gamma_x} \tag{12}$$

where e_{mn} are scattering parameters of the error model.

Fig. 7. Error 3-port as a model of the measurement system for calibration and measurement correction.

This equation can be rewritten into more general form as

$$T_{21} = \frac{C_1 + C_2\Gamma_x}{1 - C_3\Gamma_x} \tag{13}$$

where

$$C_1 = e_{21}, \tag{14}$$

$$C_2 = e_{31}e_{23} - e_{21}e_{33}, \tag{15}$$

$$C_3 = e_{33}. \tag{16}$$

The corrected value of the reflection coefficient of the DUT can be then calculated as

$$\Gamma_x = \frac{T_{21} - C_1}{C_2 + C_3T_{21}}. \tag{17}$$

A calibration is performed by using three fully known 1-port calibration standards with reflection coefficients $\Gamma^{(1)}$, $\Gamma^{(2)}$ and $\Gamma^{(3)}$ consecutively connected at the test port in place of the DUT. The calibration constants C_1, C_2 and C_3 can be then obtained as a solution of a system of three linear equations (13) for the three unknowns C_1, C_2 and C_3. The solution is given by (18)-(20), where $T^{(i)}$ is the measured transmission coefficient T_{21} when a calibration standards with reflection coefficient $\Gamma^{(i)}$ is connected in place of the DUT.

$$C_1 = \frac{T^{(1)}T^{(2)}\Gamma^{(3)}\left(\Gamma^{(2)} - \Gamma^{(1)}\right) + T^{(1)}T^{(3)}\Gamma^{(2)}\left(\Gamma^{(1)} - \Gamma^{(3)}\right) + T^{(2)}T^{(3)}\Gamma^{(1)}\left(\Gamma^{(3)} - \Gamma^{(2)}\right)}{T^{(1)}\Gamma^{(1)}\left(\Gamma^{(2)} - \Gamma^{(3)}\right) + T^{(2)}\Gamma^{(2)}\left(\Gamma^{(3)} - \Gamma^{(1)}\right) + T^{(3)}\Gamma^{(3)}\left(\Gamma^{(1)} - \Gamma^{(2)}\right)} \tag{18}$$

$$C_2 = \frac{T^{(1)}T^{(2)}\left(\Gamma^{(1)} - \Gamma^{(2)}\right) + T^{(1)}T^{(3)}\left(\Gamma^{(3)} - \Gamma^{(1)}\right) + T^{(2)}T^{(3)}\left(\Gamma^{(2)} - \Gamma^{(3)}\right)}{T^{(1)}\Gamma^{(1)}\left(\Gamma^{(2)} - \Gamma^{(3)}\right) + T^{(2)}\Gamma^{(2)}\left(\Gamma^{(3)} - \Gamma^{(1)}\right) + T^{(3)}\Gamma^{(3)}\left(\Gamma^{(1)} - \Gamma^{(2)}\right)} \tag{19}$$

$$C_3 = \frac{T^{(1)}\left(\Gamma^{(2)} - \Gamma^{(3)}\right) + T^{(2)}\left(\Gamma^{(3)} - \Gamma^{(1)}\right) + T^{(3)}\left(\Gamma^{(1)} - \Gamma^{(2)}\right)}{T^{(1)}\Gamma^{(1)}\left(\Gamma^{(2)} - \Gamma^{(3)}\right) + T^{(2)}\Gamma^{(2)}\left(\Gamma^{(3)} - \Gamma^{(1)}\right) + T^{(3)}\Gamma^{(3)}\left(\Gamma^{(1)} - \Gamma^{(2)}\right)} \tag{20}$$

Calibration of the VNA itself is not necessary, since its imperfections are covered by the error 3-port model. Despite of calibration and correction imperfections of the real measurement system cause that the reference reflection coefficient Γ_{ref} is moved from its originally designed position in the complex plane. For broadband operation, this generally means that the measured value T_{21} moves back from the center of the complex plane T_{21} reducing applicable gain of the amplifier and sensitivity of the measurement system.

The calibration coefficients C_1 and C_2 can be used to define a useful tool for qualifying the quality of the measurement system hardware – an effective reference reflection coefficient $\Gamma_{ref,eff}$. It is a reflection coefficient of the DUT resulting in zero measured transmission coefficient T_{21}. From (17) we see that

$$\Gamma_{ref,eff} = \Gamma_x \big|_{T_{21}=0} = -\frac{C_1}{C_2}. \qquad (21)$$

The effective reference reflection coefficient indicates how far from the center of the complex plane T_{21} the measurement system is actually operated.

From the effective reference reflection coefficient $\Gamma_{ref,eff}$ an effective reference impedance $Z_{ref,eff}$ can be calculated using (1). For proper operation of the measurement system with high sensitivity the effective reference impedance $Z_{ref,eff}$ should be very close to the impedance Z_x that we want to measure ($Z_x \approx Z_{ref,eff}$).

3. Experimental Results

An experimental verification of the proposed measurement method was performed on a measurement system configured for measurement of high impedances. The measurement system comprises a subtracting passive 4-port network (180deg 3dB hybrid coupler) and an open end as the reference impedance – i.e. the measurement system setup C in Tab. 1.

In the first part of the experimental verification improvement of the measurement system stability, theoretically predicted by (9), is proved and compared with classical method of impedance measurement by the VNA. In the second part results of experimental measurement of resistive impedances ranging from 12 kΩ up to 330 kΩ are provided.

3.1 Measurement Stability Improvement

Reduction of uncertainty of the measured reflection coefficient Γ_x described by (9) was experimentally verified and compared with the classical method of impedance measurement by measuring the reflection coefficient of the DUT directly by the VNA.

A fully warmed up VNA Agilent PNA E8364A was calibrated for classical reflection coefficient measurement by Open-Short-Load method at the end of an SMA female-female adaptor connected at the end of VNA's flexible test cable Agilent 85133. Male calibration standards (offset) Open, (offset) Short and Broadband Load from Agilent 85052C 3.5mm Precision Calibration Kit were used [7].

Subsequently, during 94 minutes the VNA in CW mode collected $N = 3201$ values of the measured reflection coefficient Γ_x of an open end of the female SMA connector (i.e. high impedance DUT). The measurement was done at frequency 1.57 GHz, which is the frequency that was used in the second part of this experiment. IF bandwidth was set to 1 Hz and a generator power level was set to -7 dBm. Room temperature did not change more than (29.5 ± 0.5) ˚C.

To show spreading of the measured values of the reflection coefficient Γ_x of the DUT around an average value an operator ρ calculating a distance of a data point d_i, $i = 1, 2, ..., N$ from the average value was defined as

$$\rho[d_i] = d_i - \frac{1}{N}\sum_{j=1}^{N} d_j. \qquad (22)$$

The $N = 3201$ points $\rho[\Gamma_x]$ are depicted in a polar plot in Fig. 9. The average measured value was $\Gamma_{x,\,AVG} = 1.005 \llcorner -0.96$˚. However, absolute accuracy of this value is not too important for this experiment.

In the second part of the experiment the same measurement was done by the developed measurement method. Arrangement of the measurement system is depicted in Fig. 8.
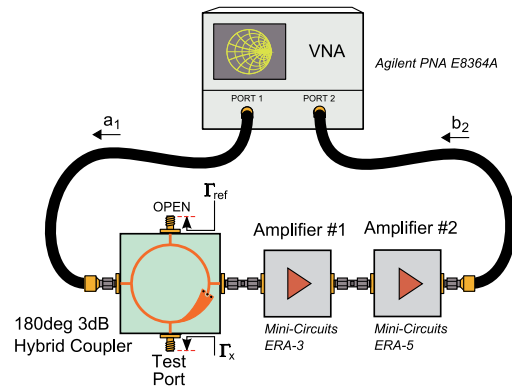
Fig. 8. Arrangement of the measurement system for verification the measurement stability improvement.
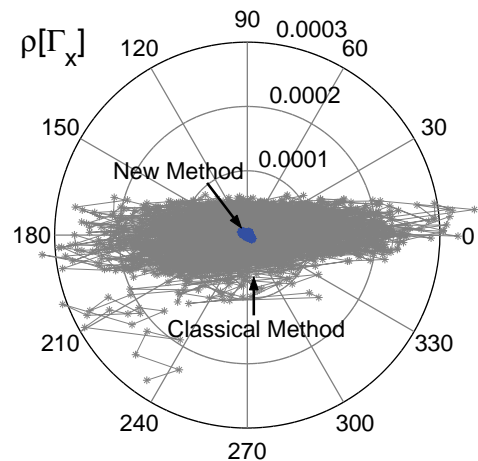
Fig. 9. Spreading of the 3201 values of the measured reflection coefficient Γ_x of the SMA female open end (high impedance DUT) around the average value calculated by (22) at frequency 1.57 GHz – comparison of the classical method and the proposed method.

Microstrip 180degree 3dB hybrid coupler with phase inverter was used. The reference arm was terminated

simply by SMA female open end of the SMA flange connector of the coupler. Two amplifiers with ICs Mini-Circuits ERA-3 and ERA-5 [8], providing overall gain 35.27 dB (G = 58.01) at the operating frequency, were used. The VNA was used for measurement of the transmission coefficient T_{21}. No correction of the VNA itself was applied.

The measurement was done at frequency 1.57 GHz, which is the frequency where the measured transmission coefficient T_{21} reaches its minimum – the reference reflection coefficient Γ_{ref} and the reflection coefficient Γ_x of the DUT are mutually very well subtracted. Generator power level was set to -40 dBm. The rest of the conditions remained the same.

The measurement system was calibrated by the same 1-port calibration standards (offset) Open, (offset) Short and Load at the test port (i.e. one of the ports of the hybrid coupler – see Fig. 8). However, it should be noted that Open-Short-Load calibration technique is not suitable for this method since principle of subtraction of the reference and the measured reflection coefficient will not work well for at least two of the three calibration standards. More-over, in the case of the Agilent 85052C calibration kit calibration standards Open and Short do not provide open end termination and short termination in the reference planes because they are offset calibration standards. There-fore, the generator power level must be set to a sufficiently low value to ensure that amplifiers operate in small signal region even during the calibration, where the measured $|T_{21}|$ are high for Short and Load calibration standards.

Spreading of the corrected values of the reflection coefficient Γ_x of the female open end of the SMA flange connector of the hybrid coupler (high impedance DUT) is depicted in Fig. 9. The average value of the calculated reflection coefficient Γ_x is $\Gamma_{x,AVG}$ = 1.001 ∟ -0.91˚. How-ever, absolute accuracy of this value is not too important for this experiment.

By using the proposed method the radius of the area, where all the measured values $\rho[\Gamma_x]$ lie decreased more than 26-times. That is in good agreement with (9), since the overall voltage gain of the amplifiers is G = 58.01, the constant $|A| \approx 2$ (due to the 3dB hybrid coupler) and the measurement accuracy of the VNA for the reflection coefficient (classical method) was nearly the same as for the transmission coefficient (new method). That results in ratio G/A = 26.

The experiment proved that the developed method is capable of outstanding measurement stability improvement which is necessity for measurement of extreme imped-ances.

3.2 Results of Extreme Impedances Measurement

This subsection describes a real measurement of sev-eral SMD resistors of size 0603 with values ranging from 12 kΩ up to 330 kΩ. These values can be absolutely con-sidered as extreme impedances.

An arrangement of the measurement system is de-picted in Fig. 10 and a photo is shown in Fig. 11.
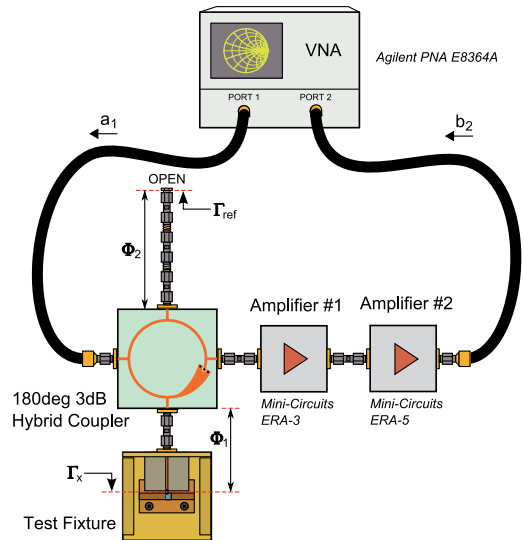
Fig. 10. Arrangement of the measurement system for measurement of extreme impedances of SMD resistors.

Most of the arrangement is the same as in the experi-ment described in section 3.1. Only the reference and the test branch were modified.

In the test branch of the hybrid coupler a microwave test fixture for measurement of SMD components was connected. Electrical length from the port of the hybrid coupler to a reference plane of the measurement, lying in the position of the SMD resistor, is Φ_1.

In the reference branch an open-ended coaxial line formed by male-male and female-female SMA adaptors was used. Electrical length of this line is Φ_2. At the operat-ing frequency $\Phi_2 \approx \Phi_1$.
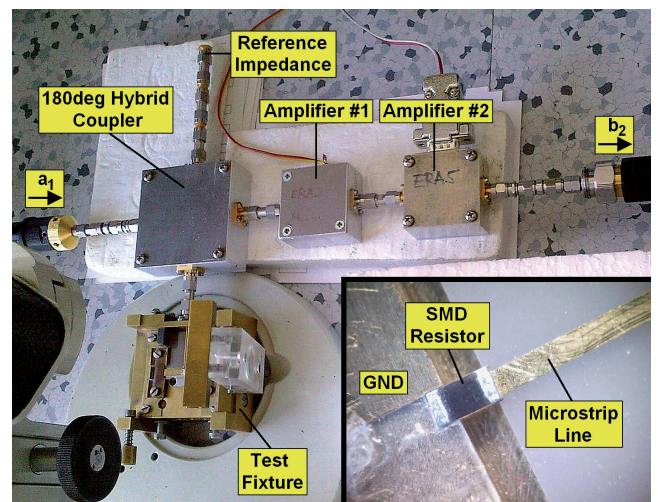
Fig. 11. Photo of the measurement system configured for meas-urement of extreme impedances of SMD resistors – the inset shows an SMD resistor in the opened test fixture.

Measurements were performed in CW mode at frequency 1.80 GHz. This is the frequency where the measured transmission coefficient T_{21} reaches its minimum – the reference reflection coefficient Γ_{ref} and the reflection coefficient Γ_x are mutually very well subtracted. At this frequency the overall gain of the amplifiers is 35.03 dB ($G = 56.41$). A generator power level was set to -40 dBm, IF bandwidth was set to 10 Hz and 101 points were acquired during 8.94 seconds in each measurement. For all calculations an average value of the 101 measured values of the transmission coefficient T_{21} was used.

Calibration of the measurement system was performed by a new calibration technique using three different resistors. SMD resistors of the same size 0603 with values 11 kΩ, 76 kΩ and 1 MΩ were used for calibration. These values were chosen so that they describe an area of the Smith chart where the measured impedances lie.

Moreover, using these high values of resistors causes that magnitude of the measured transmission coefficient T_{21} does not change too much during calibration. Thus, non-linearities of the amplifiers as well as nonlinearities of the receivers of the VNA do not have any significant effect on accuracy of the results.

By using the SMD resistors of the same dimensions as the calibration standards as well as the DUTs and de-scribing the standards as purely resistive impedances by their DC resistance the parasitics of the SMD resistors become an integral part of the error model and they are eliminated by calibration and correction. Thus, in ideal case, when the parasitics of all the SMD resistors are the same, the measured values of impedances of the resistors can be expected to be purely real impedances.

The DC resistance of the used resistors was assumed to be the true value of their impedance and in the case of the calibration standards it was used for their description.

Results of the measurements are in Tab. 2. The results exhibit reasonable agreement between the measured values of extreme impedances and the DC resistance values of the SMD resistors up to 240 kΩ.

However, for higher resistor values the values of the measured impedances differ significantly from the sup-posed (DC) values. It was experimentally determined that the connection reproducibility of the used test fixture ranges from 3.3E-5 to 1.3E-3. Therefore, it can be sup-posed that these measurements are affected by the limited connection reproducibility of the used test fixture.

Fig. 12 shows the properties of the measurement method for general complex impedances of the DUT.

It depicts a conformal mapping (13) – impedance grid for the impedance Z_x of the DUT – in the complex plane of the measured transmission coefficient T_{21} calculated from the calibration coefficients C_1, C_2 and C_3 obtained from the calibration by the SMD resistors 11 kΩ, 76 kΩ and 1 MΩ. The conformal map is depicted in for impedances Z_x rang-ing from 10 kΩ up to 100 kΩ, respectively ∞, with step 10 kΩ in both the real and the imaginary part.

DUT	DC Resistance (kΩ)	Measured Impedance	
		Re[Z_x] (kΩ)	Im[Z_x] (kΩ)
Cal. std. 1	11.00	–	–
1	12.01	13.16	1.13
2	12.97	13.45	-0.21
3	16.08	14.84	-0.79
4	18.57	19.17	-2.70
5	22.23	24.90	-0.83
6	26.87	31.18	1.15
7	34.08	35.88	0.09
8	42.50	38.45	3.82
9	52.10	56.56	11.01
10	62.10	61.66	12.26
Cal. std. 2	75.70	–	–
11	90.70	92.74	3.58
12	99.30	79.43	-11.56
13	150.20	132.50	-4.12
14	239.70	208.80	-6.79
15	329.50	202.36	323.39
Cal. std. 3	1004.00	–	–

Tab. 2. Results of measurement of extreme impedances of SMD resistors of size 0603 ranging from 12 kΩ up to 330 kΩ at frequency 1.80 GHz.
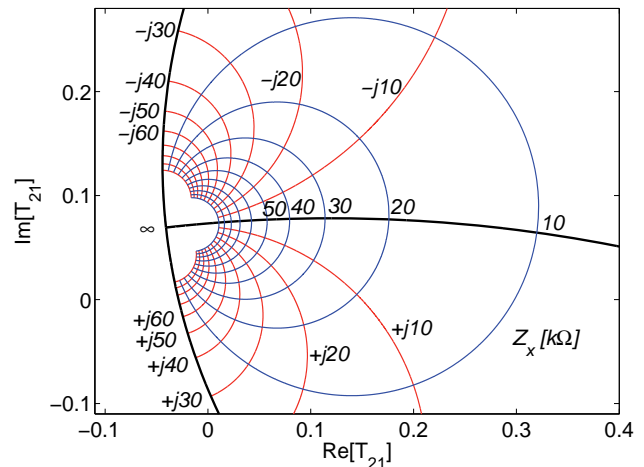
Fig. 12. Conformal mapping – impedance grid for the impedance Z_x of the DUT in the complex plane of the measured transmission coefficient T_{21} at frequency 1.80 GHz for impedances Z_x ranging from 10 kΩ up to 100 kΩ, respectively ∞, with step 10 kΩ.

The calculated effective reference reflection coefficient (21) is $\Gamma_{ref,eff} = 0.999 \llcorner -0.08°$ and the corresponding effective reference impedance is $Z_{ref,eff} = (22.66 + j59.58)$ kΩ indicating very good configu-ration of the measurement system for measurement of extremely high impedances.

4. Conclusion

A method for measurement of extremely high and extremely low impedances was introduced. The method is based on either adding or subtracting of the reference reflection coefficient and the reflection coefficient of the

DUT by a passive 4-port network and measuring an amplified version of the resulting signal by a common VNA as a transmission coefficient.

The measurement method was successfully experimentally verified. The method provides outstanding measurement sensitivity to value of impedance of the DUT and significantly reduces effects of drift and noise of the VNA compared to the classical method. Experimental measurement of extremely high impedances was shown and the corresponding impedance grid in the complex plane of the measured transmission coefficient was calculated.

The proposed measurement method represents a significant contribution to microwave metrology for the fast growing field of nanoelectronics.

Acknowledgements

References

[1] McEUEN, P. L., FUHRER, M. S., PARK, H. Single-walled carbon nanotube electronics. *IEEE Transactions on Nanotechnology,* 2002, vol. 1, no. 1, p. 78 - 85.

[2] BURKE, P. J., YU, Z., LI, S, RUTHERGLEN C. Nanotube technology for microwave applications. In *Proceedings of the MTT-S International Microwave Symposium*. Long Beach (CA, USA), 2005, p. 12 - 17.

[3] MOSLEY, L. E. Capacitor impedance needs for future microprocessors. In *Proceedings of the CARTS USA 2006 Conference*. Orlando (FL, USA), 2006.

[4] BRYANT, G. H. *Principles of Microwave Measurements*. Revised ed. Stevenage: Peter Peregrinus, 1993.

[5] RICHTER, M., TANBAKUCHI, H., WHITENER, M. Design of scanning capacitance microscope. In *Proceedings of the 68th ARFTG Microwave Measurement Symposium*. Broomfield (CO, USA), 2006.

[6] BAHL, I., BHARTIA, P. *Microwave Solid State Circuit Design*. 2nd ed. Hoboken: Wiley, 2003.

[7] Agilent Technologies, USA. *Specifying Calibration Standards and Kits for Agilent Vector Network Analyzers (application note)*. 42 pages. [Online] Cited 2010-09-21. Available at: http://www.cp.literature.agilent.com/litweb/pdf/5989-4840en.pdf.

[8] Mini-Circuits, USA. *Amplifiers – Surface Mount Monolithic Gain Blocks (selection guide)*. [Online] Cited 2010-09-21. Available at: http://www.mini-circuits.com/products/ /amplifiers_monolithic.html.

About Authors ...

Martin RANDUS was born in Prague, Czech Republic, in 1981. He received the Ing. degree (Hons.) in electrical engineering from the Czech Technical University in Prague, Czech Republic, in 2007. He is currently with the Dept. of Electromagnetic Field of the Faculty of Electrical Engineering at the Czech Technical University in Prague, where he is working towards the Ph.D. degree. His research interests include microwave measurements, especially new techniques for measurement of extreme impedances, and microwave active and passive circuits.

Karel HOFFMANN was born in Prague, Czech Republic. He graduated from the Czech Technical University in Prague, Faculty of Electrical Engineering, in 1974 (Hons.). He was named Associate Professor in 1993 and Professor in 2002 with the Czech Technical University in Prague, Faculty of Electrical Engineering. His professional activities are focused on active and passive microwave integrated circuits, correction methods for precise microwave measurement, microwave vector network analyzers and modeling of microwave components. He was a Chairman of the MTT/AP/ED joint chapter of the Czechoslovak section of IEEE in 1999.